INSTITUTE OF GEOLOGICAL SCIENCES
GEOPHYSICAL DIVISION

GLOBAL SEISMOLOGY UNIT

G.S.U. REPORT 86

Magnitude Determination on Lownet

by

A.W.B. Jacob and G. Neilson

June 1977

MURCHISON HOUSE
WEST MAINS ROAD
EDINBURGH EH9 3LA
(Tel. 031-667 1000)

Magnitude Determination on LOWNET

by A. W. B. Jacob and G. Neilson

GS830263X

Introduction

Routine processing of seismic signals observed on LOWNET involves making measurements of (1) time and (2) amplitude and period. The time measurements contribute to a determination of the source position and origin time while the amplitude/period measurements allow a determination of its magnitude. The determination of source position and origin time is relatively straightforward relying on accuracy of onset timing and phase identification and a clear statement of which earth model is used.

The position with magnitudes had always been rather more confused and there are a number of magnitude scales in general use. This report describes the methods of magnitude determination used on LOWNET, compares LOWNET results with those from the world network, and finally makes some attempt to link some of the scales using data from LOWNET plus some neighbouring stations. The results should be relevant to other networks set up within Britain. Finally some magnitude/charge size plots for quarries and underwater explosions are shown and briefly discussed.

Magnitude Scales

There are four magnitude scales used on LOWNET. They are as follows:

(1) M_L Richter Local Magnitude

(2) M_b Magnitude determined from teleseismic P waves

(3) M_s Magnitude determined from surface wave data

(4) M_b^* a scale which attempts to measure M_b at short range

(1) The Richter Local Magnitude (Richter 1935) as originally used was very limited and the equation for M_L referred to measurements on the recorded trace amplitude of a standard Wood-Anderson instrument sited in Southern California. In his paper Richter says 'Precision in this matter was neither expected nor required'. He wanted only to be able to segregate large, moderate and small earthquakes and it was left to later workers to get entangled in the problems that greater precision and expectations produced. As it is used at present M_L is defined by

$$M_L = \log_{10}A - \log_{10}A_o$$

where A is the recorded trace amplitude for an earthquake at a given distance as written by a Standard Torsion Seismometer and A_o is the amplitude that would be recorded on the same instrument at the same range from a 'standard earthquake' which is thus defined as having a magnitude $M_L = 0$ (Richter 1958). Values of $-\log A_o$ are given in Table 1 (taken from Richter 1958).

The application of this scale to LOWNET raises at least three problems. The first is that the amplitude response of LOWNET is not the same as that of the standard Wood-Anderson system. A correction can be applied to the maximum amplitude observed on a LOWNET station to convert it to the amplitude a Wood-Anderson would have recorded at the period observed but this is not necessarily the maximum amplitude a Wood-Anderson system would have given for that earthquake at that site, because of its different response. The second problem is that at only one site (EDI) are there horizontal seismometers (see map in Fig. 1). The third problem is that Scotland is not Southern California and differences in A_o might be expected.

Of all these problems the first is probably the most serious. Thatcher (1973) has pointed out that magnitude scales for classifying local earthquakes are frequently related to Richter's M_L but that the precise relationship between M_L and other scales is often quite unclear. The primary cause is the difference in the shape of the amplitude response curve and the fact that the two systems may produce two very different seismograms for the same event with the maximum amplitude at a different frequency and position in each. Thatcher considers that 'it would be preferable to have spectrum measurements over a range of magnitudes in order to understand precisely the relationships between different magnitude scales and make it possible to tie them together accurately'. We have simply taken the maximum amplitude observed on our seismograms to determine "M_L" for LOWNET. Thatcher considered that such a course would supply an 'adequate tie-in with any other magnitude scale used in a given region'.

The second problem was dealt with in one study using LOWNET (Crampin et al, 1972) by applying a correction so as to allow the use of data from vertical seismometers at outstations but generally only results from EDI have been used.

The fact that velocity structure and average Q in Scotland and in Southern California are not the same should affect the value of Log A_o and ideally a distance/log A_o scale should be constructed for this area, but there is probably not enough data available yet to establish a local A_o scale. Richter's scale has thus been used and M_L values used to compare with M_b^* have been computed with that scale (see later).

(2) The body wave magnitude, M_b, is determined from the amplitude and period of the P wave arrival at ranges usually in excess of 20°. It is probably most reliable beyond 30°.

$$M_b = \log A/T + \sigma(\Delta) + S$$

A is the amplitude in microns, T the period in seconds for the maximum swing in the first few cycles. The correction factors, $\sigma(\Delta)$, used for LOWNET are obtained from a table in the "Manual of Seismological Observatory Practice" (see Table 2). S in the equation is a term which may include corrections for non-average source surroundings, wave-path, and station surroundings. It is normally set to zero but, as heterogeneity of the earth certainly has a marked effect on the registered magnitude, attempts have been made to measure such corrections and to link them to earth structure (see the work of P.D. Marshall and many others for such considerations in both M_S and M_b). The equation is the basis of magnitude determinations in the output of the NEIS and the ISC Bulletin. However most of the data used by these organizations is based on short-period, narrow band instruments (e.g. LOWNET) and this has the result that the maximum value observed for M_b is not normally above 7. This is because the source frequency spectrum changes as magnitude increases so that at higher magnitudes amplitude measurements are being made at frequencies well removed from the source peak. This problem should not arise if wide-band instruments are used. These have long been used in Russia and are now becoming more common elsewhere. Fig. 12 shows the dominant period of the P wave for earthquakes and nuclear explosions measured on a wide-band system. The Russians also contend that it is better to measure the maximum amplitude in the first 20 or 25 seconds and not to restrict the measurements to the first few cycles.

(3) The Surface Wave Magnitude M_S is calculated using what is essentially the same equation

$$M_S = \log(A/T) + \sigma(\Delta) + S$$

where $$\sigma(\Delta) = 1.66 \log\ ^{\circ} + 3.3$$

This second equation is the Prague-Moscow 1962 formula. The amplitude and period are measured at the maximum of the phase (usually on the LP-Z component) but it is recommended that waves used should not have periods shorter than certain values (see the Manual of Seismological Observatory Practice). The only LOWNET M_S measurements have been based on the broad-band system.

(4) The M_b^* scale is one which attempts to measure the equivalent of M_b at ranges as short as 200 km. The equation we use is

$$M_b^* = \log V + 2.3 \log R - 2$$

where V is the ground velocity represented by the maximum trace amplitude in the P wave train in microns per second and R is the distance in km. The asterisk in M_b^* is a convention we have adopted to show that though it is a value calculated to be equivalent to M_b it is not derived in the usual way. The equation is derived from work in the United States by Navarro and Brockman (1970). Initially this was used (for instance in Jacob and Willmore 1972) without any adjustment for British or overall average European conditions. Since then we have more data to make a local check on it. Within the limits of experimental error it seems to hold remarkably well.

The main source for checking the equation and making a comparison with genuine teleseismic values was the 10 ton shot programme. Some of the data were presented to the ESC in Brazov (Jacob and Willmore 1974) but a larger data set has since become available. Where the equation is written as

$$M_b^* = \log V + A \log R + B$$

values have been found as follows

$$A = 2.4 \pm 0.2 \qquad B = -2.1 \pm 0.5$$

This result was based on 62 amplitude readings from European stations and 17 values of M_b obtained at teleseismic range. As these coefficients are not significantly different from those in the equation used earlier its use has been continued and all M_b^* values have been based on the original equation. These results show remarkably good agreement with the United States ones but it should be remembered that the relationship is based on near surface explosions and need not necessarily apply to deep sources. There is not enough data to make a full check for near earthquakes, but a few near LOWNET which have also been observed at teleseismic range have been measured, the results are in Table 3 and plotted in Fig. 3. The line shown is that which would hold if there were an exact 1:1 relationship. The only result which needs any comment is number 5. The LOWNET M_b^* was 6.9 against an NEIS value of $M_b = 6.1$. A study of the EDR showed that not only was there a large scatter of M_b values from individual stations but that a number of stations in Europe at a similar azimuth to LOWNET and at a distance greater than 20° gave similar high values. Examples were GRF 7.1, PRU 6.9, STU 6.9.

Comparison of LOWNET results with those from the world network

The results of a comparison between M_b determined on individual LOWNET stations and the NEIS values are shown in Table 4 and plots of residuals (M_b(NEIS) - M_b(LOWNET) are shown in fig 4. There is not a significant variation with range for the data shown and the data for each station have been put together to give an average station magnitude correction. For instance, the correction to be applied to the EDU readings is -0.2 which means that amplitudes on the Dundee station are usually large. The average residual for the whole of LOWNET is -0.04 which is effectively zero. Most of the events were not at great depth and no depth corrections were made. Usually a magnitude is determined quickly in response to enquiries about a major or damaging event and in most cases no information is initially available about depth. The range of the event is best determined by the S-P interval (a broad-band system, recently installed at EDI, is very useful for this if the event is large and distant) with a bearing gained from the arrival pattern on LOWNET. The phase velocity calculated from the first arrival pattern also gives a check on the range.

All these measurements for M_b were made in the manner recommended for input to NEIS and ISC, i.e., measurements were made on the first few cycles of the P-wave train. If the maximum amplitude in the first 20 seconds is taken then the measured A/T will sometimes be larger. Fig. 5 shows the plot of some measurements in the range $4.8<M_b<7.0$. Calling the 20 second measurement M_{bR} we find that its value may be up to 0.5 greater than M_b. The one very big difference was observed for a North Atlantic event ($M_{bR} - M_b = 1.1$).

Since the broad system has been working on a routine basis measurements of M_s have been made. A plot of M_s EDI versus M_s NEIS for events in 1976 (to 16/8/76) is shown in fig. 6. The line is drawn on the assumption of a 1:1 relationship. The response curves for the broad band system are shown in fig. 7. The average residual M_s NEIS - M_s EDI is -0.1 Though the scatter is large the indications are that the station correction for EDI is effectively zero (as it is for M_b measurements).

Comparison of Magnitude Scales

These comparisons come into two categories. The first depends mainly on data from the world network (e.g. M_b/M_s and M_b^*/M_b). The second includes only local magnitude determinations, in our case the comparison between M_L and M_b^*.

M_b and M_s

Until quite recently LOWNET did not provide measurements of surface wave amplitude and period so it was not possible to give M_s magnitudes to enquirers. As it is the Richter surface wave magnitude which is usually quoted in radio, TV, and newspaper reports (because it is normally bigger?) a means of approximately converting M_b to M_s was sought. Many papers have been written on the relationship between M_b and M_s and the most recent comparison is that made by Kondorskaye using ISC data (almost the same as NEIS from whom they got most of their amplitude information). She found that

$$M_s = 2.119 M_b - 5.826 \qquad \ldots\ldots\ldots\ldots\ (1)$$

P. Marshall (1970) obtained an almost identical relationship

$$M_s = 2.08 M_b - 5.65 \qquad \ldots\ldots\ldots\ldots\ (2)$$

which was based on PDE values. A regional set was obtained in Canada by Basham (1969)

$$M_s = 1.18 M_b - 0.51 \qquad \ldots\ldots\ldots\ldots\ (3)$$

An earlier equation was that given by Gutenberg and Richter

$$M_s = 1.59 M_b - 3.97 \qquad \ldots\ldots\ldots\ldots\ (4)$$

Prozorov and Hudson (1974) used a large body of data to produce a relation

$$M_s = 1.92 M_b - 4.76 \quad \ldots\ldots\ldots\ldots\ldots (5)$$

but this involved weighting the raw data to allow for errors in determination of M_b and M_s and a straightforward regression line through their data without this refinement gave

$$M_s = 1.06 M_b - 0.17 \quad \ldots\ldots\ldots\ldots (6)$$

All these equations assume that the relationship between M_s and M_b is linear but an interesting diagram is shown by Evernden (1975, p.367) where the graph is certainly not linear. We have plotted the lines resulting from these equations in fig. 7. While there are considerable differences between some of them it should be remembered that they are based mostly on data $4<M_s<8$ and in some cases a much narrower range than that. There is not enough data to plot any M_b/M_s LOWNET values but fig. 8 and fig. 9 are drawn from NEIS sources with Kondorskaye's line superimposed show how well actual observations fit the conversion formula. Fig. 9 is drawn from data for the North Atlantic ocean, mainly events associated with ridges. M_b/M_s may be slightly lower for ridge events due to a very low Q environment at the source but the effect is not very marked on the plot.

M_L and M_b^*

We have made comparisons between M_L and M_b^* for events observed by LOWNET. This comparison is useful because, though their ranges of applicability overlap, one cannot be used to the exclusion of the other. M_L can be used from 0 km though as distance increases any discrepancy between Richter's A_o values and those that should be used in Britain will have greater impact. No attempt has yet been made to measure the variation of A_o with distance but as the available data increases it may become realistic to determine this parameter. M_b^* is linked to a teleseismic scale but does not work well for distances less than 200 km. The reason for this is connected with rapid variations in amplitude of PmP and other reflected phases within the crust at such short ranges. McMechan and Workman (1974), considering the distance range 10^o to 35^o, have found that maximum amplitude arrivals show less model dependence than first arrivals in the same wave trains and, while the M_b^* scale is taken to shorter ranges, the same holds quite well in the 2^{o} to 10^{o} range in this area.

Fig. 10 shows M_L versus M_b^* for British earthquakes observed on LOWNET. The lower magnitude end of the scale is fixed by the fact that $M_b^* = 2$ is about the LOWNET detection threshold for 200 km and the upper limit is decided by the lack of larger earthquakes in Britain since LOWNET commenced operations. The regression line through the set of 43 values gives

$$M_L = 0.72 M_b^* + 1.0$$

This line is also plotted in fig. 11 which shows the comparison of M_L and M_b^* for underwater explosions. For a given M_b^* the explosions register a lower M_L but tend to fall more nearly on the earthquakes line at greater magnitudes. Apart from the fact that earthquakes aught to generate relatively more S waves one may note that the smaller shots may show a reduced M_L value because they are high frequency sources and losses due to anelastic absorption are probably significant (Q_s being lower than Q_p). It is worth noting that the event at M_b^* 2.5/M_L 2.2 was a particularly low frequency source (period 0.8 seconds) and gave a higher M_L than the other values $M_b^* < 3$ which were smaller but more efficient sources generating higher frequencies (period 0.2 seconds approx.).

Magnitude versus size of explosion

The first plot (fig. 13) is mainly drawn from the literature and shows an interesting comparison between the efficiency of optimum depth water shots and other sources. There appear to be three populations here and three lines have accordingly been drawn.

(1) The least efficient are the large nuclear blasts.

(2) More efficient are smaller chemical blasts in water and on land (though 2 nuclear blasts get into this category). The Lake Superior shots fall into this group too as they were mostly not at optimum depth.

(3) IGS optimum depth shots with corrected values for LISPB dispersed shots included.

With the exception of the optimum depth data results of this kind appear in the writings of such authors as Evernden. In fig. 13 one can note a tendency for all these lines to converge so that it appears that at really large yields the nature of the explosion and its environment lose their importance. The figures for some of the smaller optimum depth shots are drawn from M_b^* results (the 0.2 tonne Minol charges for example), and the apparent yield of the dispersed shots is calculated on the basis of an average range of 300 km from LOWNET and Q = 1000. The actual efficiency of the dispersed shots at such short range is, of course, even greater than appears on fig. 13 but the correction makes the comparison with normal optimum depth shots valid.

Fig. 14 is a plot of M_L against charge size for underwater explosions. The higher values are all associated with refraction experiments where some attempt has been made to maximixe the efficiency. The group of lower M_L, through which a line has been drawn, give results for explosions generally fired in shallow water and in many cases the shot will have vented. The one large explosion in this set, the demolition of the St. Bridget, lies close to the projection of the line through the group of smaller shots and the tendency to converge with the more efficient set appears to be present here too.

Fig. 15 is included to show the enormous scatter in results from quarry blasts and their generally low efficiency as seismic sources. Variations will generally be caused by differences in the rock being quarried and in the methods of firing. Delay methods, such as ripple blasting, are extremely inefficient from a seismic point of view.

References

Basham, P. Canadian magnitudes of earthquakes and nuclear explosions in S.W. North America, Geophys. J.R. Astr. Soc., 17, 1 (1969).

Crampin, S., Jacob, A.W.B., Neilson, G. The Glenalmond earthquake series, February 1970-March 1972, Nature, 240, 233-236, (1972).

Crampin, S., Jacob, A.W.B., Miller, A., and Neilson, G. The LOWNET radio-linked Seismometer Network in Scotland, Geophys. J.R. Ast. Soc., 21, 207-216 (1970).

Evernden, J.F. Further Studies on seismic discrimination, B.S.S.A., 65, 359-391 (1975).

Gutenberg, B. and Richter, C.F. Magnitude and energy of earthquakes, Annali Geofis., 9, 1-15 (1956).

Jacob, A.W.B. and Willmore, P.L. Teleseismic P-waves from a 10 ton explosion, Nature, 236, 305-306 (1972).

Jacob, A.W.B. and Willmore, P.L. 10 ton explosions fired in 1971 and 1972, Proc. XIII General Assembly E.S.C., Brazov, Part II, 329-337 (1974).

Kondorskaye, N.V. Magnitude Determinations at the International Seismological Centre, unpublished report, May 1975.

McMechan, G.A., and Workman, W.G. P-Wave amplitudes and magnitudes between 10° and 35°, B.S.S.A., 64, 1887-1899 (1974).

Marshall, P.D. Aspects of the Spectral Differences between earthquakes and underground explosions, Geophys. J.R. Astr. Soc., 20, 397-416 (1970).

Marshall, P.D., and Basham, P.W. Discrimination between earthquakes and underground explosions exploying an improved M_S scale, Geophys. J.R. Astr. Soc., 28, 431-458 (1972).

Navarro, R. and Brockman, F.R. New Rulison Test Site, USCGS Pub. No. 746-5 (1970).

Prozorov, A., and Hudson, J.A. A study of the magnitude difference M_S-M_b for earthquakes, Geophys. J.R. Astr. Soc., 39, 551-564 (1974).

Richter, C.F. An instrumental earthquake magnitude scale, B.S.S.A., 25, 1-32 (1935).

Richter, C.F. Elementary Seismology, publ. W.H. Freeman & Co., London, 1958.

Thatcher, W. A Note on discrepancies between local magnitude (M_L) and microearthquake magnitude scales, B.S.S.A., 63, 315-319 (1973).

Willmore, P.L. and Karnik, V. Manual of seismological observatory practice, published by International Seismological Centre, Edinburgh, 1970.

Burton, P W 1974. 'An array of broad band seismographs: Some initial results'. Proceedings of the XIVth General Assembly of the European Seismological Commission, Trieste, September 1974 (Editor H Stiller, Published Berlin 1975).

Tables

Figures

TABLE 1

Table 1 Logarithms of the Amplitudes A_o (in millimeters) with which a Standard Torsion Seismometer (T_o = 0.8, V = 2800, h = 0.8) Should Register an Earthquake of Magnitude Zero

Δ (km)	$-\log A_o$	Δ (km)	$-\log A_o$	Δ (km)	$-\log A_o$
0	1.4	150	3.3	390	4.4
5	1.4	160	3.3	400	4.5
10	1.5	170	3.4	410	4.5
15	1.6	180	3.4	420	4.5
20	1.7	190	3.5	430	4.6
25	1.9	200	3.5	440	4.6
30	2.1	210	3.6	450	4.6
35	2.3	220	3.65	460	4.6
40	2.4	230	3.7	470	4.7
45	2.5	240	3.7	480	4.7
50	2.6	250	3.8	490	4.7
55	2.7	260	3.8	500	4.7
60	2.8	270	3.9	510	4.8
65	2.8	280	3.9	520	4.8
70	2.8	290	4.0	530	4.8
80	2.9	300	4.0	540	4.8
85	2.9	310	4.1	550	4.8
90	3.0	320	4.1	560	4.9
95	3.0	330	4.2	570	4.9
100	3.0	340	4.2	580	4.9
110	3.1	350	4.3	590	4.9
120	3.1	360	4.3	600	4.9
130	3.2	370	4.3		
140	3.2	380	4.4		

TABLE 2

Table 3.2 AMPLITUDE FACTORS $\sigma(\Delta)$ FOR SHALLOW SHOCKS

Δ°	PZ	PH	PPZ	PPH	SH
16	5.9	6.0			7.2
17	5.9	6.0			6.8
18	5.9	6.0			6.2
19	6.0	6.1			5.8
20	6.0	6.1			5.8
21	6.1	6.2			6.0
22	6.2	6.3			6.2
23	6.3	6.4			6.2
24	6.3	6.5			6.2
25	6.5	6.6			6.2
26	6.4	6.6			6.2
27	6.5	6.7			6.3
28	6.6	6.7			6.3
29	6.6	6.7			6.3
30	6.6	6.8	6.7	6.8	6.3
31	6.7	6.9	6.7	6.8	6.3
32	6.7	6.9	6.8	6.9	6.4
33	6.7	6.9	6.8	6.9	6.4
34	6.7	6.9	6.8	6.9	6.5
35	6.7	6.9	6.8	6.9	6.6
36	6.6	6.8	6.7	6.8	6.6
37	6.5	6.7	6.7	6.8	6.6
38	6.5	6.7	6.7	6.8	6.6
39	6.4	6.6	6.6	6.7	6.7
40	6.4	6.6	6.6	6.7	6.7
41	6.5	6.7	6.5	6.6	6.6
42	6.5	6.7	6.5	6.6	6.5
43	6.5	6.7	6.6	6.7	6.5
44	6.5	6.7	6.7	6.8	6.5
45	6.7	6.9	6.7	6.8	6.5
46	6.8	7.1	6.7	6.8	6.6
47	6.9	7.2	6.7	6.8	6.6
48	6.9	7.2	6.7	6.8	6.7
49	6.8	7.1	6.7	6.8	6.7
50	6.7	7.0	6.7	6.8	6.6
51	6.7	7.0	6.7	6.8	6.5
52	6.7	7.0	6.7	6.8	6.5
53	6.7	7.0	6.7	6.8	6.6
54	6.8	7.1	6.8	6.9	6.6
55	6.8	7.1	6.9	7.0	6.6
56	6.8	7.1	6.9	7.0	6.6
57	6.8	7.1	6.9	7.0	6.6
58	6.8	7.1	7.0	7.1	6.6
59	6.8	7.1	7.0	7.2	6.6
60	6.8	7.1	7.1	7.3	6.6
61	6.9	7.2	7.2	7.4	6.7
62	7.0	7.3	7.3	7.4	6.7
63	6.9	7.3	7.3	7.4	6.7
64	7.0	7.3	7.3	7.5	6.8
65	7.0	7.4	7.3	7.5	6.9
66	7.0	7.4	7.3	7.4	6.9
67	7.0	7.4	7.2	7.4	6.9
68	7.0	7.4	7.1	7.3	6.9
69	7.0	7.4	7.0	7.2	6.9
70	6.9	7.3	7.0	7.2	6.9
71	6.9	7.3	7.1	7.3	7.0
72	6.9	7.3	7.1	7.3	7.0
73	6.9	8.2	8.1	7.3	6.9
74	6.8	7.1	7.0	7.2	6.8
75	6.8	7.1	6.9	7.1	6.8
76	6.9	7.2	6.9	7.1	6.8
77	6.9	7.2	6.9	7.1	6.8
78	6.9	7.3	6.9	7.1	6.9
79	6.8	7.2	6.9	7.1	6.8
80	6.7	7.1	6.9	7.1	6.7
81	6.8	7.2	7.0	7.2	6.8
82	6.9	7.2	7.1	7.3	6.9
83	7.0	7.4	7.2	7.4	6.9
84	7.0	7.4	7.3	7.5	6.9
85	7.0	7.4	7.3	7.5	6.8
86	6.9	7.3	7.3	7.5	6.7
87	7.9	7.3	7.2	7.4	6.8
88	7.1	7.5	7.2	7.4	6.8
89	7.0	7.4	7.2	7.4	6.8
90	7.0	7.3	7.2	7.4	6.8
91	7.1	7.5	7.2	7.4	6.9
92	7.1	7.4	7.2	7.4	6.9
93	7.2	7.5	7.2	7.4	6.9
94	7.1	7.4	7.2	7.4	7.0
95	7.2	7.6	7.2	7.4	7.0
96	7.3	7.6	7.2	7.4	7.1
97	7.4	7.8	7.2	7.4	7.2
98	7.5	7.8	7.2	7.4	7.3
99	7.5	7.8	7.2	7.4	7.3
100	7.4	7.7	7.2	7.4	7.4
101	7.3	7.6	7.2	7.4	7.4
102	7.4	7.7	7.2	7.4	7.4
103	7.5	7.9	7.2	7.4	7.3
104	7.6	7.9	7.3	7.5	7.3
105	7.7	8.1	7.3	7.5	7.2
106	7.8	8.2	7.4	7.6	7.2
107	7.9	8.3	7.4	7.6	7.2
108	7.9	8.3	7.4	7.6	7.2
109	8.0	8.4	7.4	7.6	7.2
110	8.1	8.5	7.4	7.6	7.2
112	8.2	8.6	7.4	7.6	
114	8.6	9.0	7.5	7.7	
116	8.8		7.5	7.7	
118	9.0		7.5	7.7	
120			7.5	7.7	
122			7.4	7.6	
124			7.3	7.5	
126			7.2	7.4	
128			7.1	7.4	
130			7.0	7.3	
132			7.0	7.3	
134			6.9	7.2	
136			6.9	7.2	
138			7.0	7.3	
140			7.1	7.4	
142			7.1	7.4	
144			7.0	7.3	
146			6.9	7.2	
148			6.9	7.2	
150			6.9	7.2	
152			6.9	7.2	
154			6.9	7.2	
156			6.9	7.2	
158			6.9	7.2	
160			6.9	7.2	
170			6.9	7.2	

Annali di Geofisica 9(1956), No 1, p8.

TABLE 3

No.	Description	Δ LOWNET	M_b^*	M_b	Source
1	Iceland Region 13/1/76	12½°	5.8	6.0	NEIS
2	Kintail	2°	4.0	4.0	LAO
3	Germany, salt mine collapse, 23/6/75	9°	5.2	5.3	NEIS
4	North Atlantic, 26/5/75	23°	6.5	6.3	NEIS
5	Jan Mayen, 16/4/75	15°	6.9	6.1	NEIS
6	North West Italy, 16/11/75	12°	5.2	4.9	NEIS

TABLE 4

LOWNET M_b Magnitude Residuals

Station	Average Residual	Standard Deviation	No. of Readings
EDI	0.01	0.28	44
EAU	-0.07	0.27	53
EBH	-0.11	0.34	57
EGL	0.00	0.28	61
EAB	-0.07	0.29	60
EBL	0.10	0.30	51
EDU	-0.20	0.30	47
ELO	0.02	0.26	19

TABLE 5

M_b^* versus M_L for British earthquakes

Events	M_b^*	M_L	Events	M_b^*	M_L
North Wales	4.0	3.5	Hereford	3.6	3.5
South Wales I	3.5	3.7	Fort William	3.2	3.6
South Wales II	4.2	4.1	North Sea	4.7	3.7
Fair Isle	3.4	3.4	Manchester	2.8	2.2
Stoke	3.7	2.8	Colonsay	3.7	4.0
Kirkby-Stephen	4.0	4.2	North Sea	1.9	3.5
Anglesey	4.3	3.5	Stoke 13/5/76	2.6	2.9
Forth William	3.8	4.2	Stoke 19/5/76	2.5	1.9
Kirkby-Thore	4.4	4.9	Avon	3.3	3.0
Mansfield	3.5	3.6	Kirkby-Stephen 16/8/76	2.9	2.9
Todmorden	4.0	4.0			
Kintail	2.7	3.0			
"	3.3	3.9			
"	3.5	3.8			
"	2.7	3.0			
"	3.0	3.7			
"	4.0	4.4			
"	2.7	3.6			
"	2.5	3.0			
"	2.9	3.3			
"	2.1	3.0			
"	2.2	3.1			
"	2.7	2.8			
"	2.7	2.2			
"	3.1	2.5			
"	2.9	2.3			
"	2.7	1.9			
"	2.9	2.9			
"	2.4	2.6			
"	4.4	4.8			
"	3.0	3.8			
"	2.8	3.5			
"	2.6	2.2			

TABLE 6

M_b^* versus M_L for underwater explosions

Events			M_b^*	M_L
LISPB N11			4.0	3.0
" N21			4.4	3.3
" N24			4.5	3.3
" N25			4.5	3.5
SOSP III			3.7	3.5
" II			3.3	2.5
Tenton I			4.4	3.6
Tenton 2			4.3	4.1
Tenton 3			4.8	3.9
Cambridge	1976	50 lb.	2.9	1.5
"	"	"	2.8	1.5
"	"	"	2.8	1.7
"	"	"	3.1	1.5
"	"	200 lb.	3.4	2.7
"	"	"	3.2	2.6
Mine, West Hartlepool			2.5	2.2
Malin Head 50 lb.			2.2	1.2
HMSP 300 lb.			3.7	2.6
" "			3.6	3.0
St. Bridget 14/2/72			4.0	3.8

TABLE 7

Magnitude (M_b) versus yield

(a) Nuclear Explosions

Events	M_b	Yield Kilotons
Benham	6.3	1100
Purse	5.8	150
Salmon	4.4	5.3
Milrow	6.5	1000
Rulison	5.3	40
Gasbuggy	5.1	26
Buggy	4.1	5
Cabriolet	3.8	2.5
Longshot	5.9	80
Artesia	5.1	20
Rainer	4.1	1.8
Shoal	4.9	12
Jorum	5.1	2.5
Hardhat	4.2	5
Handcar	4.8	12
Ardvak	4.9	38
Haymaker	4.9	56
Mad	3.7	0.5
Stillwater	3.5	2.8
Doormouse II	3.6	10
Bilby	5.5	200
Chinchilla	4.2	1.8
Cimmaron	4.0	11.2
Danny Boy	3.6	0.4
Gnome	5.4	3.4

(b) Chemical on land

Events	M_b	Size (tons)
Pre-Gondola III	5.0	210
B.C. Strip mine	4.4	88
Oregon	3.9	65
Colorado	4.7	315
B.C. Strip mine	5.0	169
(c) Chemical in Water		
Post Longshot	4.5	340
"Kielce"	4.7	500
–	5.0	615
Arms Dump	4.2	5481
E. Coast U.S.	5.3	700
"	5.0	300
"	4.7	400
Lake Superior	2.9	1
"	3.0	2
"	3.2	3
"	3.3	4
"	3.5	10
(d) Optimum Depth explosions		
Tenton 1	4.2	10
Tenton 2	4.3	10.3
SOSP III	3.7	0.2
SOSP II	3.3	0.2
LISPB N11*	4.0	1.1
" N21*	4.4	5
" N24*	4.5	9.2
" N25*	4.5	11.9

*Three LISPB shots were dispersed charges and equivalent yields were calculated. Actual charges were smaller.

TABLE 8

M_L versus Charge size for Underwater explosions

Description	M_L	Charge size lbs.
Blackness, Forth	1.2	50
Society Bank, Forth	1.3	100
" " "	2.0	300
" " "	1.9	300
Dalgety Bay	1.8	300
" "	1.7	600
Pittenweem	2.0	300
off W. Hartlepool	2.2	1,500
Goxford Sands	1.7	600
Fife Ness	0.7	12
Blackness	1.1	50
"	1.6	100
Gosford Sands	1.1	328
North Sea, Cambridge project	1.9	50
" " "	1.9	50
" " "	1.7	50
" " "	2.1	50
" " "	2.7	200
" " "	2.6	200
Dalgety Bay	2.2	400
Minch, HMSP	2.6	300
"	3.0	300
off N. Ireland	1.2	50
SOSP, West Scotland	2.5	300
Tenton 1	3.6	22,000
" 2	4.1	22,600
" 3	3.9	22,000
LISPB, N11	3.0	2,500
" N21	3.3	11,000
" N24	3.3	20,000
" N25	3.5	24,000
Kirkaldy Bay	1.8	210
Dalgety Bay	2.2	750
" "	1.7	300
" "	1.8	450
" "	1.9	600
" "	2.0	900
off Wolf Rock	3.8	220,000

TABLE 9

M_L versus charge size for quarry blasts

Quarry	M_L	Charge
Westfield	0.7	1,050
"	1.0	7,700
"	0.9	5,400
Craigpark	1.4	7,320
Westfield	0.8	3,400
"	0.5	1,600
"	0.5	1,200
"	0.6	2,000
"	0.4	1,400
Craigpark	0.9	4,970
Goat	2.6	10,600
Westfield	1.5	1,060
"	1.3	1,200
"	1.7	2,600
Arroch	1.6	5,050
"	1.7	5,050
"	2.4	20,400
"	1.8	12,000
Westfield	0.7	2,800
"	0.7	700
Oxwellmains	2.4	8,408
"	1.1	6,256
"	1.4	5,270
Clatchard	1.1	535
"	1.6	800
Cunmont	2.3	3,600
Hazelbank	1.0	900
Cairngryffe	2.5	8,750
Oxwellmains	1.8	15,350
Westfield	1.4	1,200
"	1.3	1,100
"	0.7	1,050

TABLE 10 LOWNET POSITIONS

	N	W
EDI	55 55 24	3 11 10
EDU	56 32 51	3 00 51
EGL	55 51 42	2 44 18
EAB	56 11 17	4 20 24
EAU	55 50 40	3 27 17
EBH	56 14 53	3 30 29
EBL	55 46 24	3 02 37
ELO	56 28 14	3 42 43

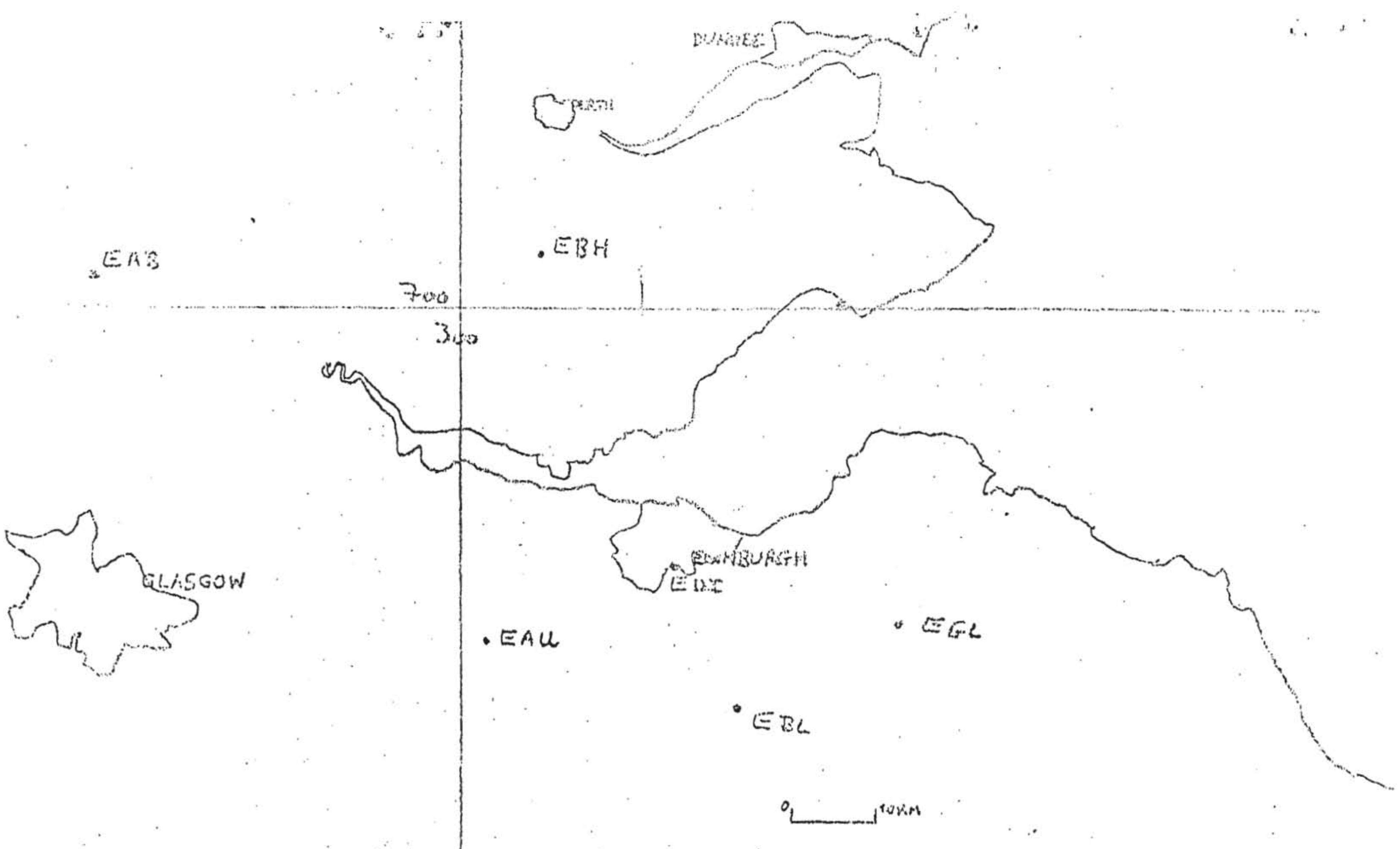
DUNDEE
PERTH
EAS
EBH
700
300
GLASGOW
EDINBURGH
EDI
EAU
EGL
EBL
0
10KM

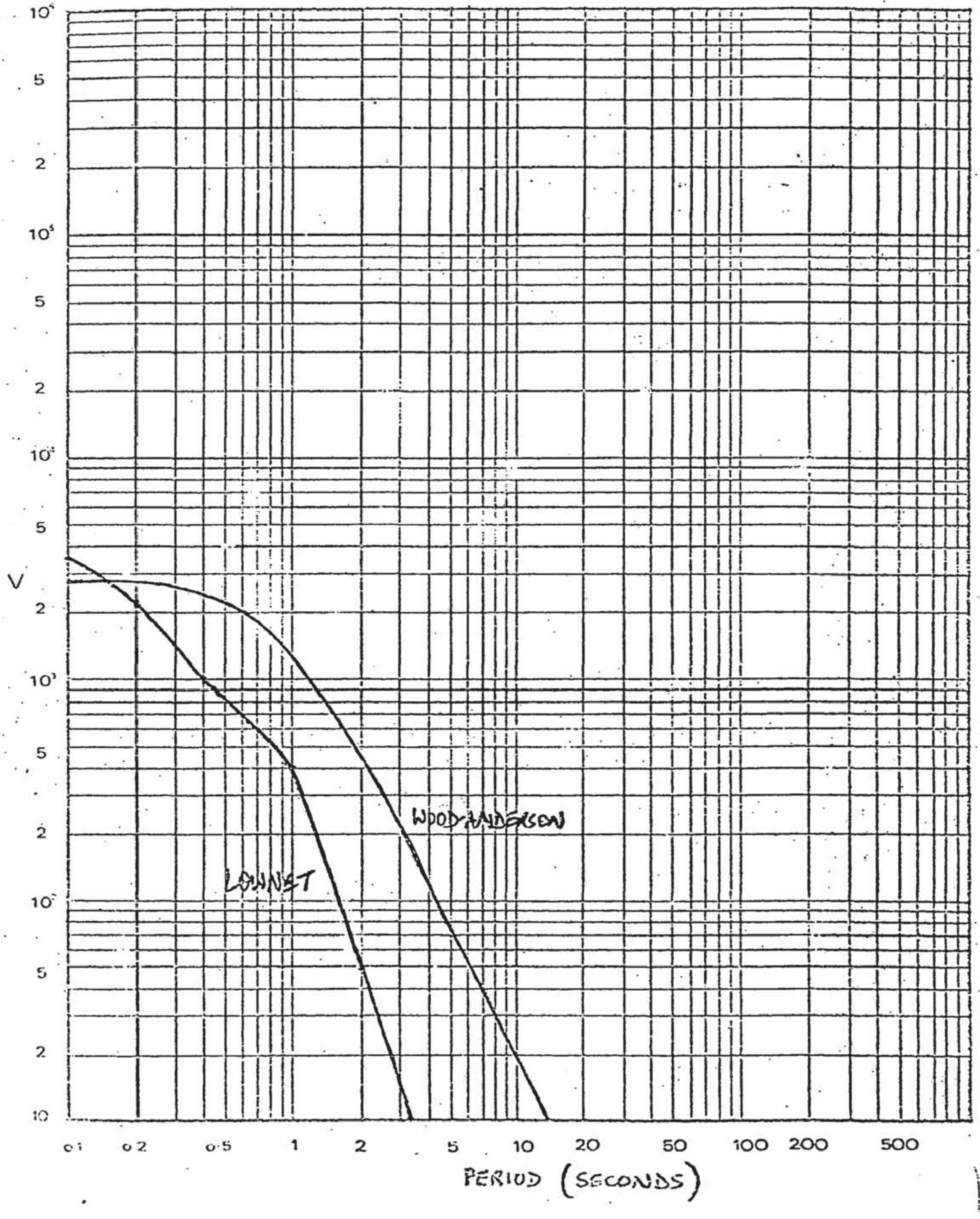
10^6
5
2
10^5
5
2
10^4
5
V
2
10^3
5
2
10^2
5
2
10
0·1
0·2
0·5
1
2
5
10
20
50
100
200
500
PERIOD (SECONDS)
WOOD-ANDERSON
LOWNET

FIG. 2

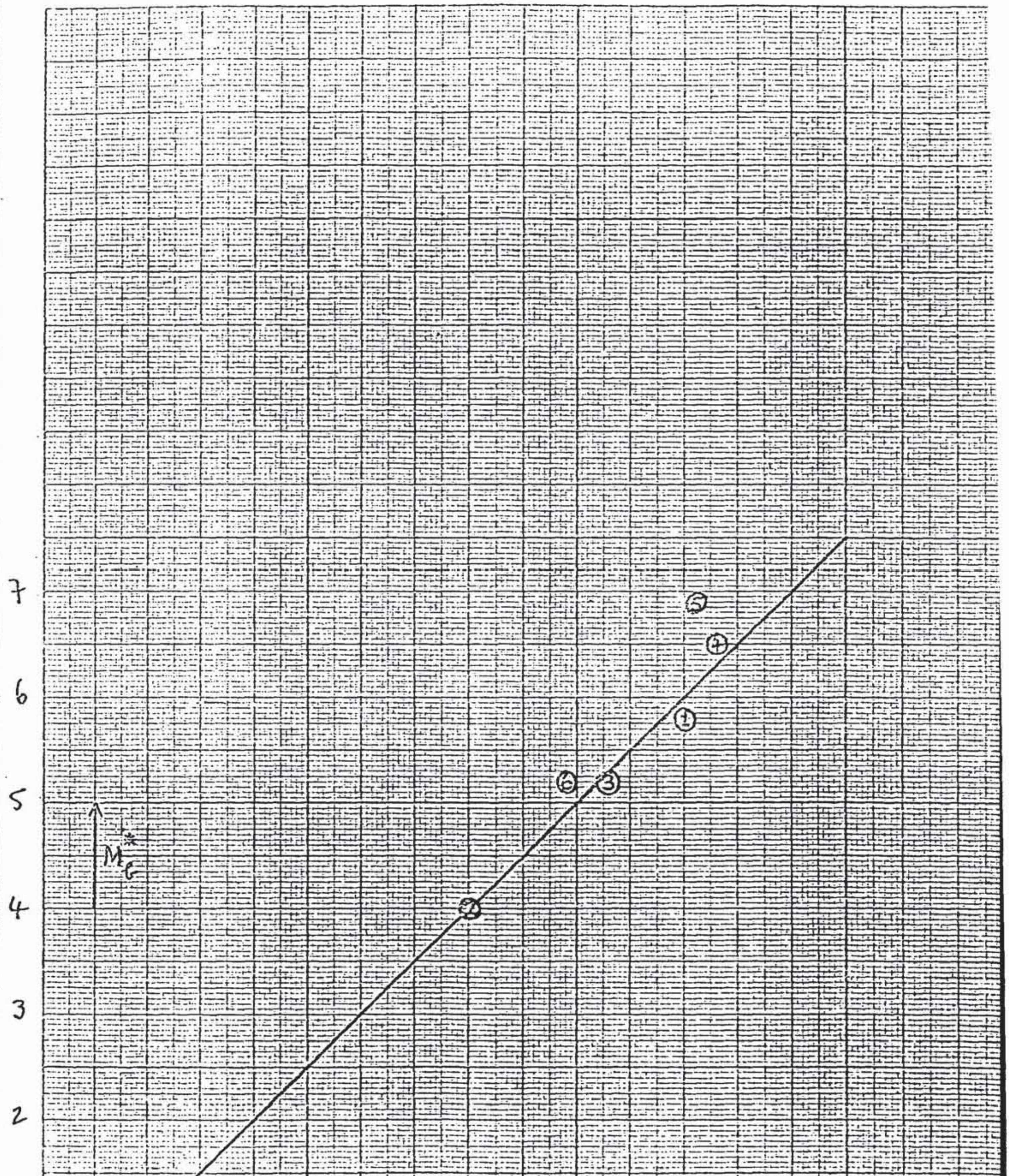

FIG. 3

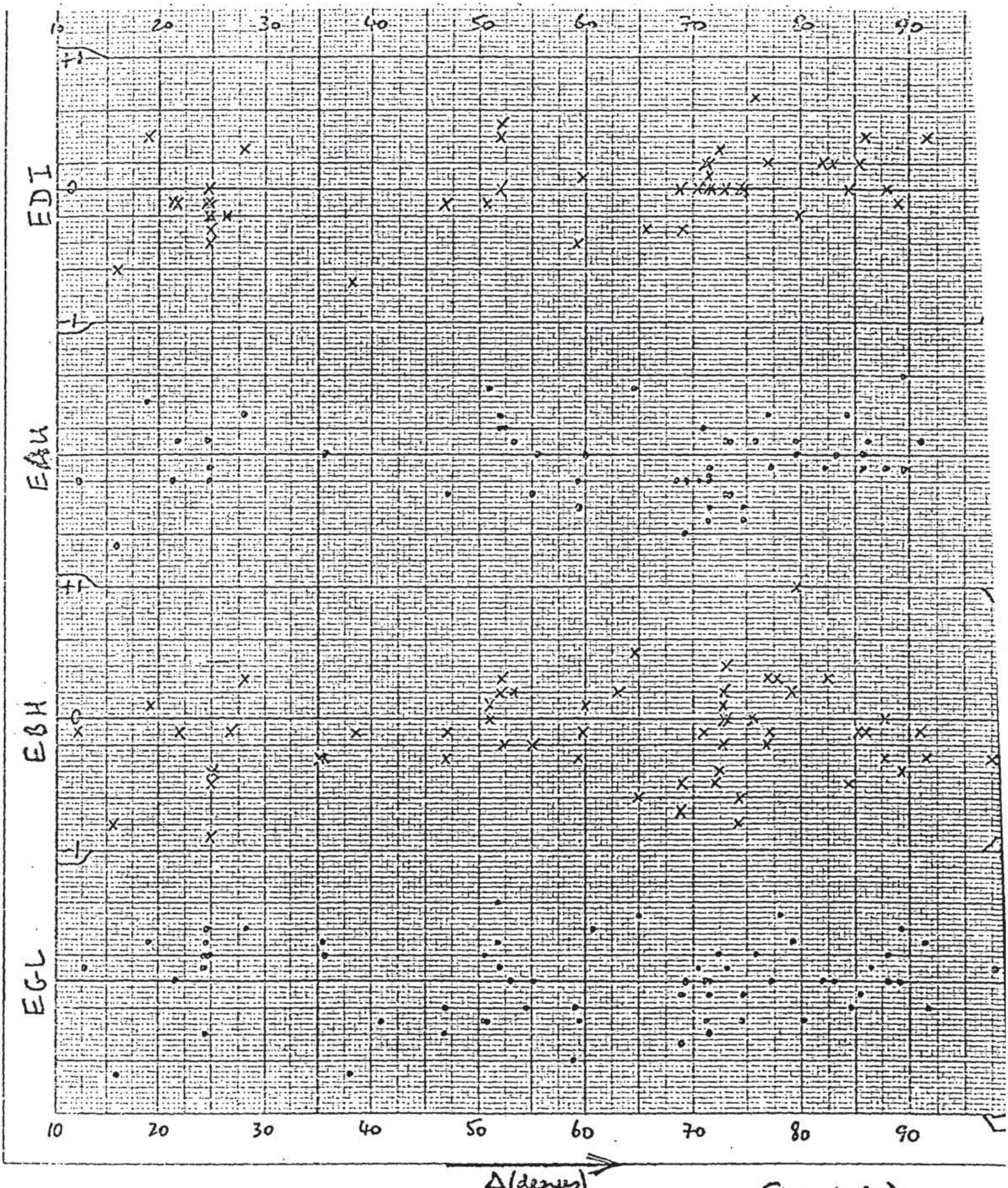

FIG. 4(a)

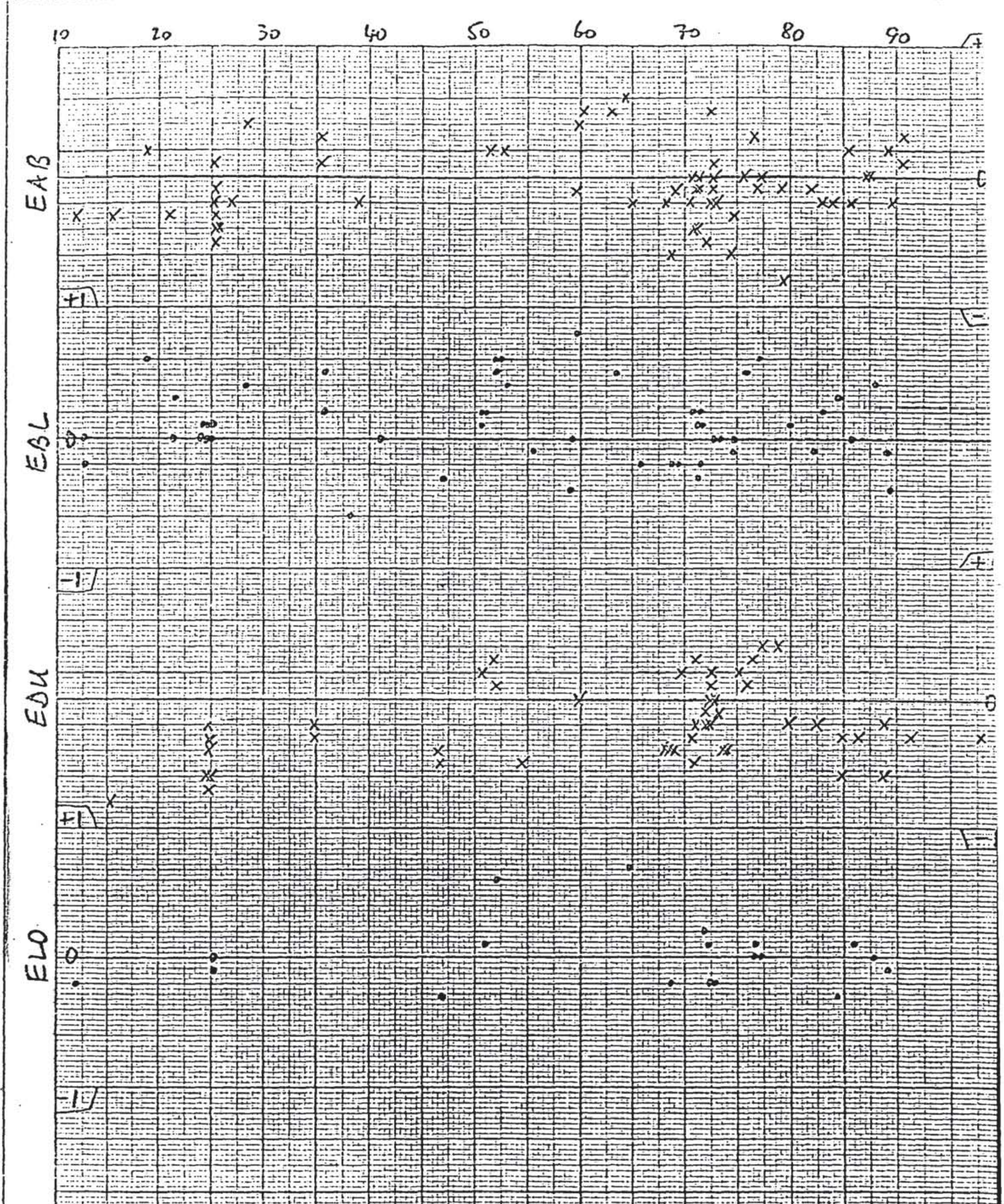
10
20
30
40
50
60
70
80
90
EAB
0
+1
EBL
0
-1
EDU
0
+1
ELO
0
-1
10
20
30
40
50
60
70
80
90
Δ(degrees)

FIG. 4(b)

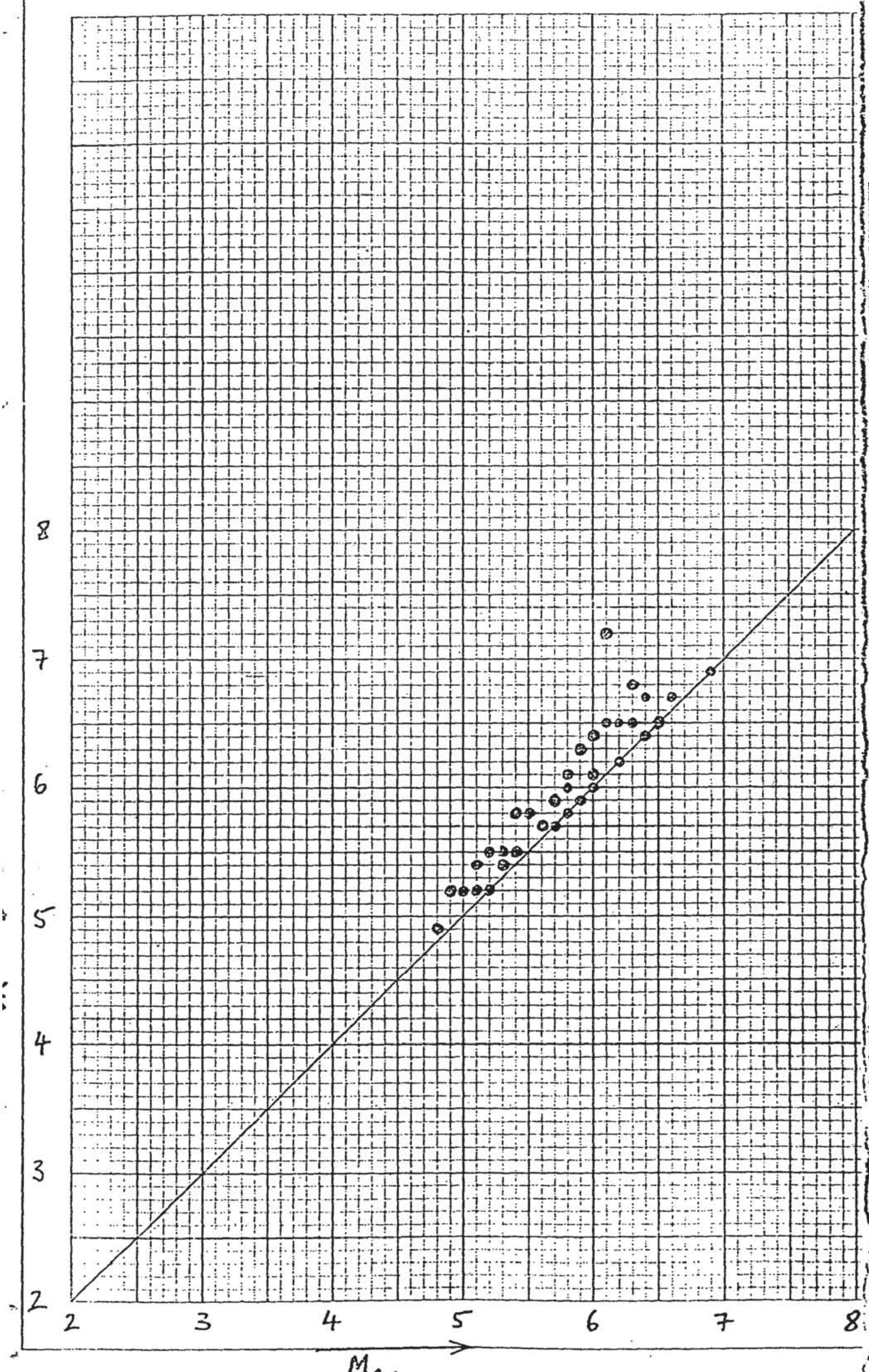

FIG. 5

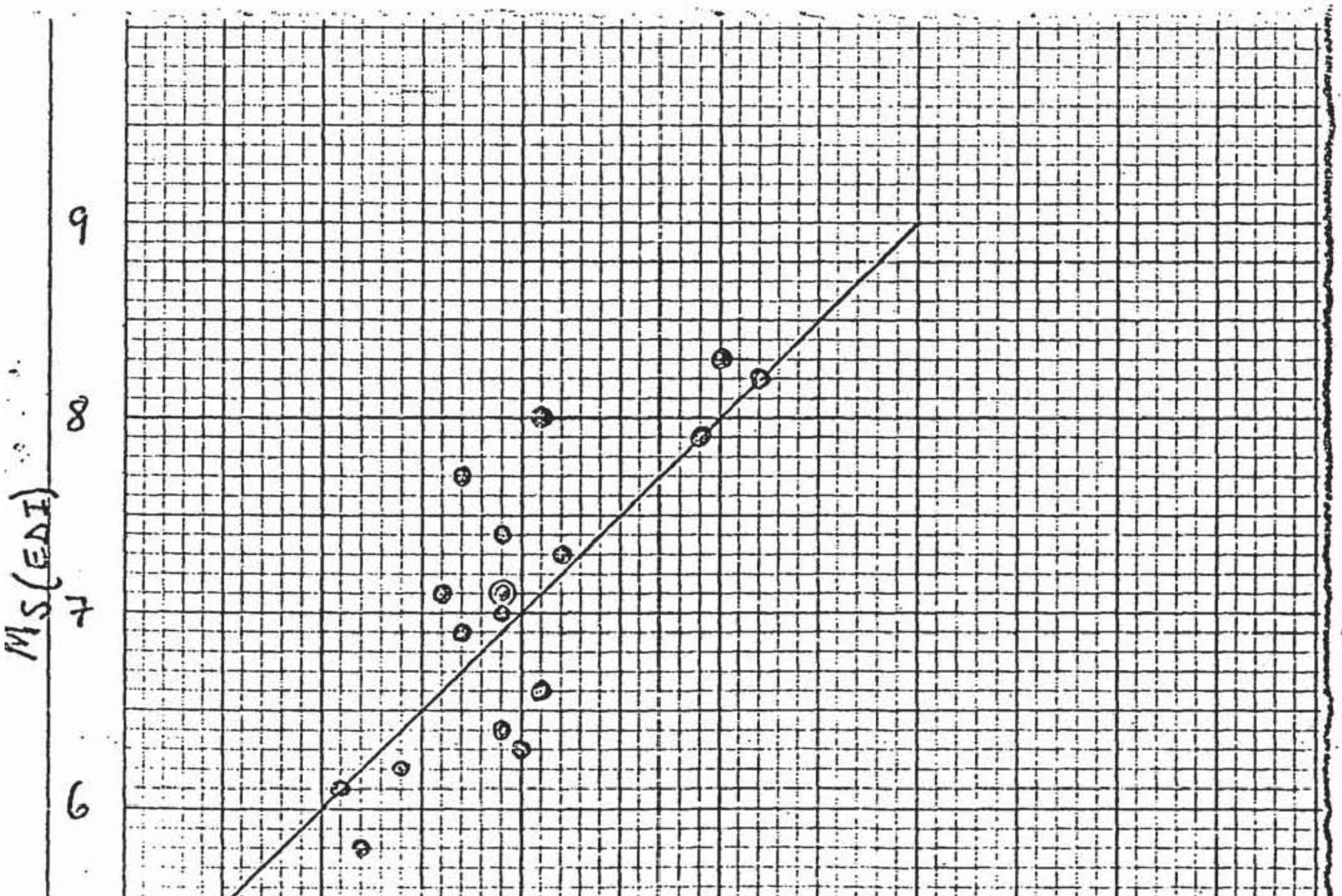

FIG. 6

LOWNET WIDE BAND SYSTEM

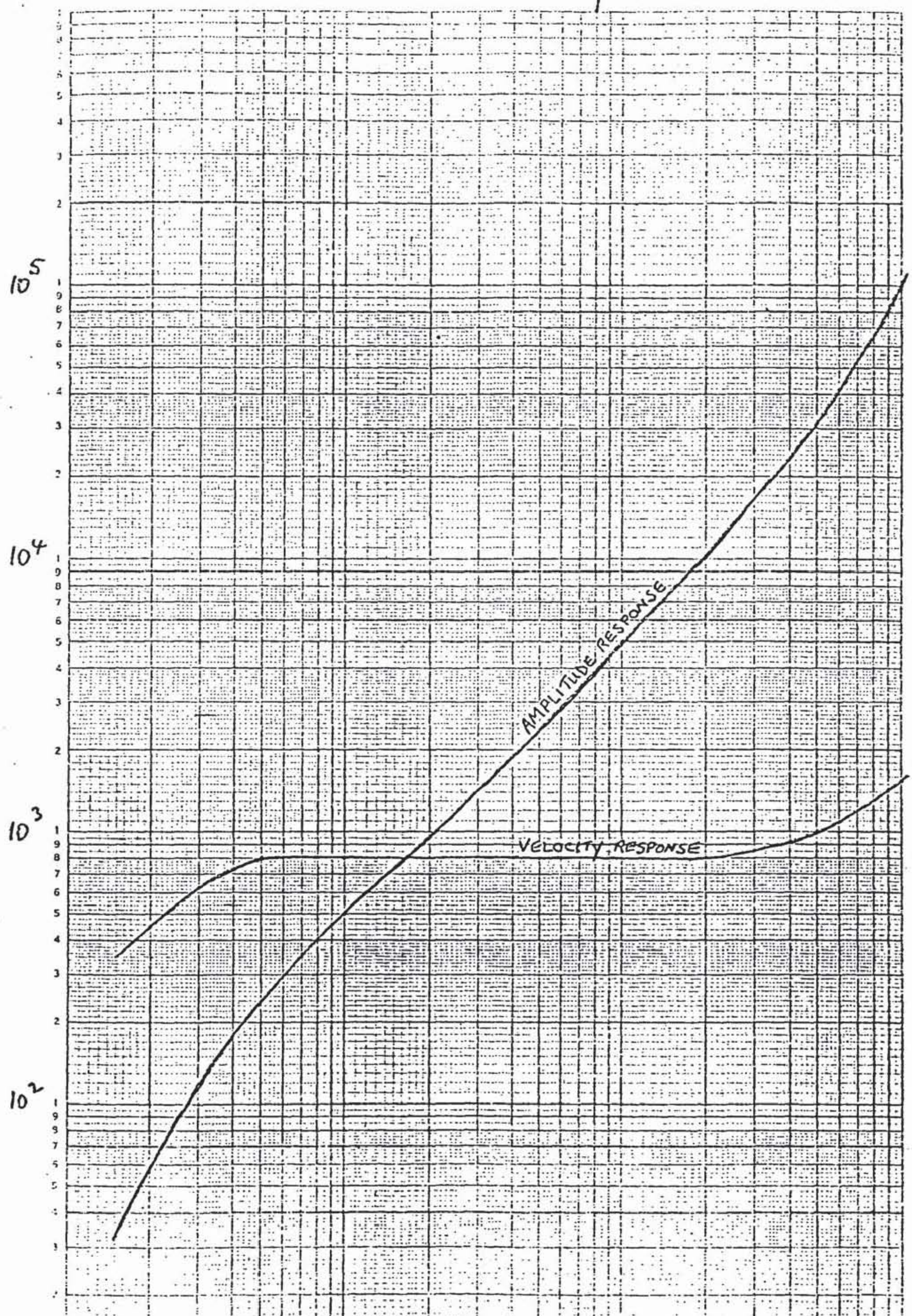

FIG. 6(a)

[illegible] meter
sits to Units)

Response of Lount T8100 S.P. System.

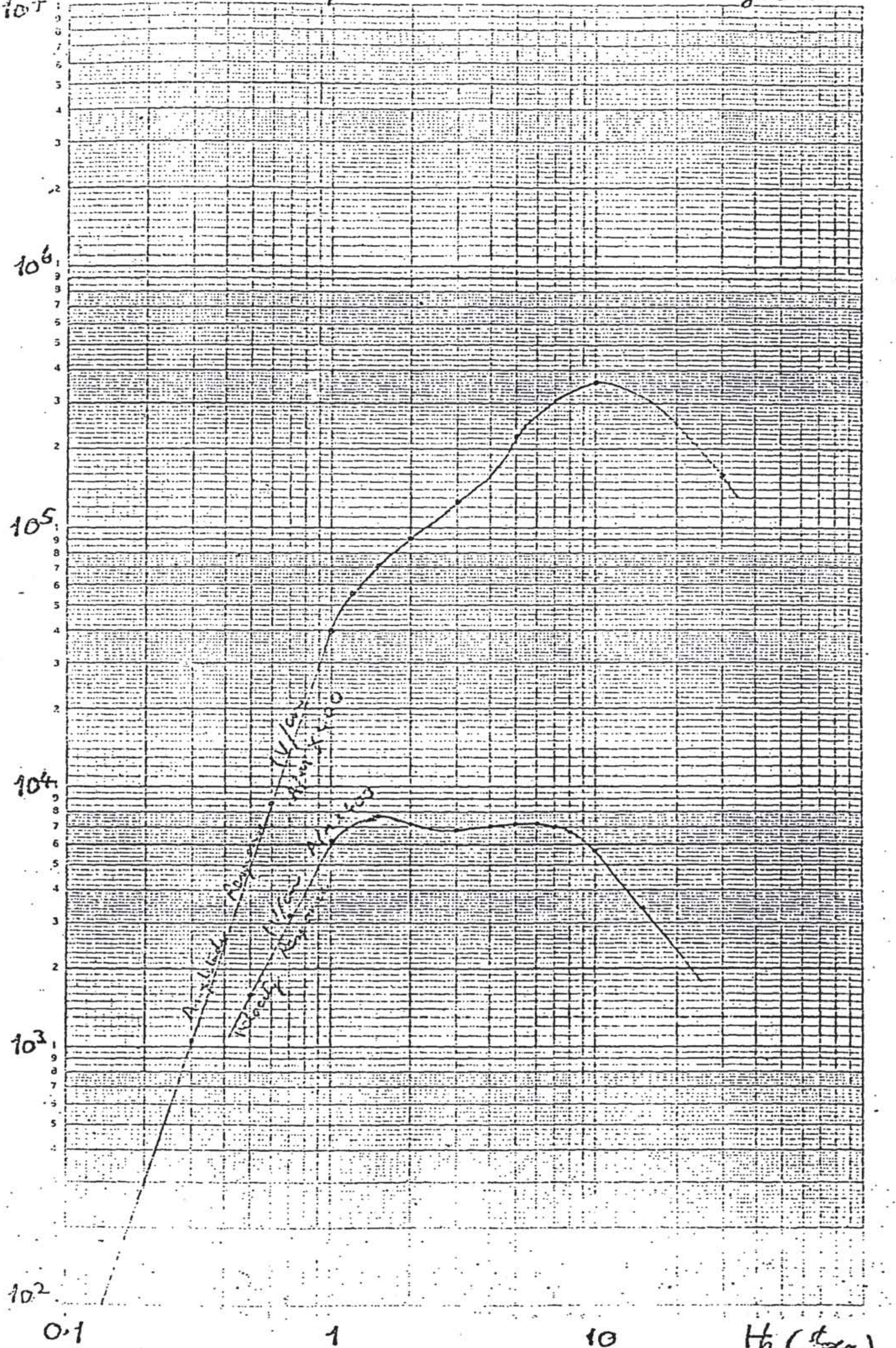

AMPLIFIER GAIN :- 400
JET PEN GAIN :- 1V/cm

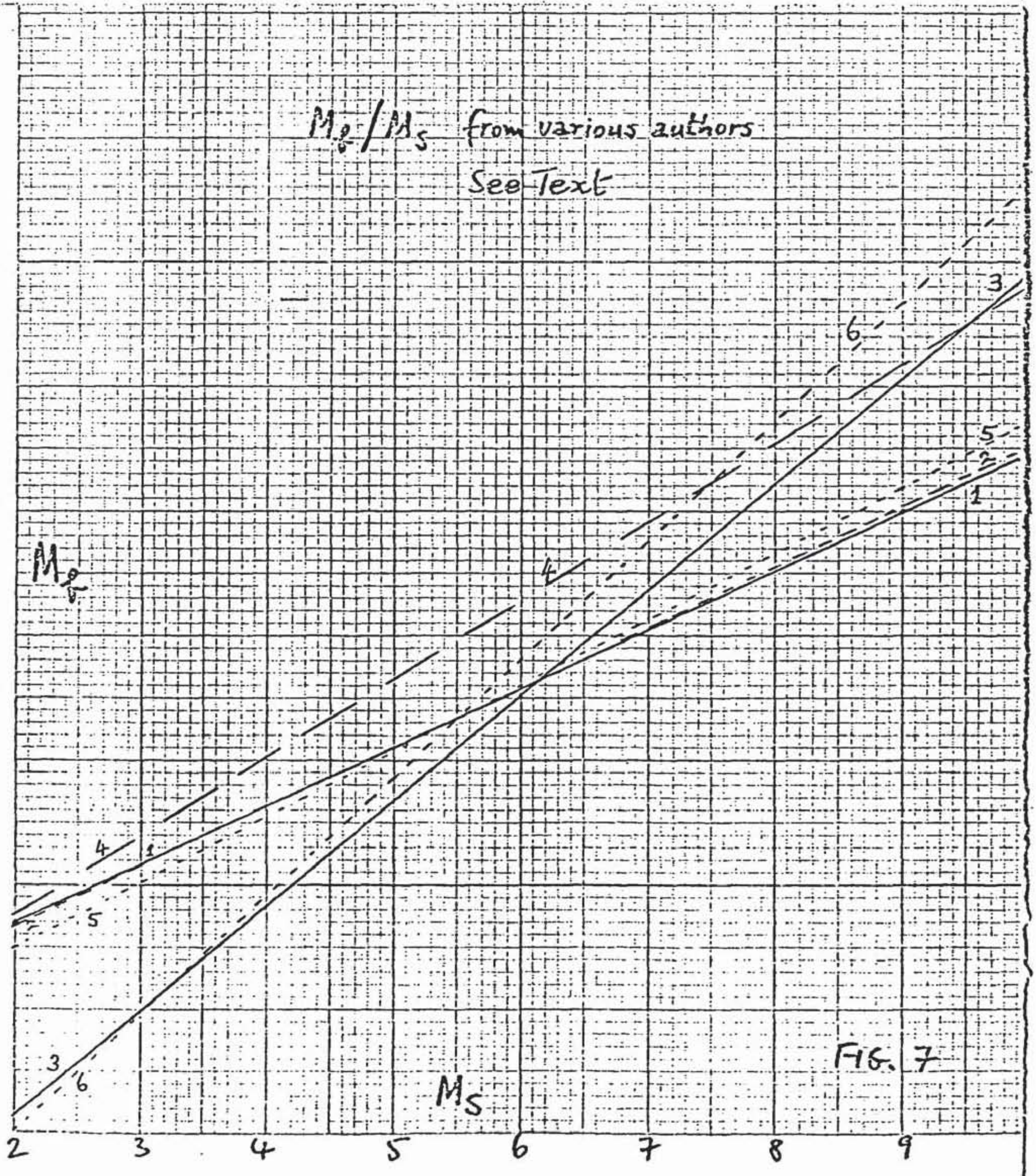

FIG. 7

M_B vs. M_S from U S G S data.

SEPT 1968 – MARCH 1969 – ALL MAGNITUDES
APRIL 1969 – SEPT 1969 – EVENTS WITH $6.0 \geq M_B \geq 6.5$
1968 – 1976 – EVENTS WITH $M_S \geq 7.0$

FIG. 8

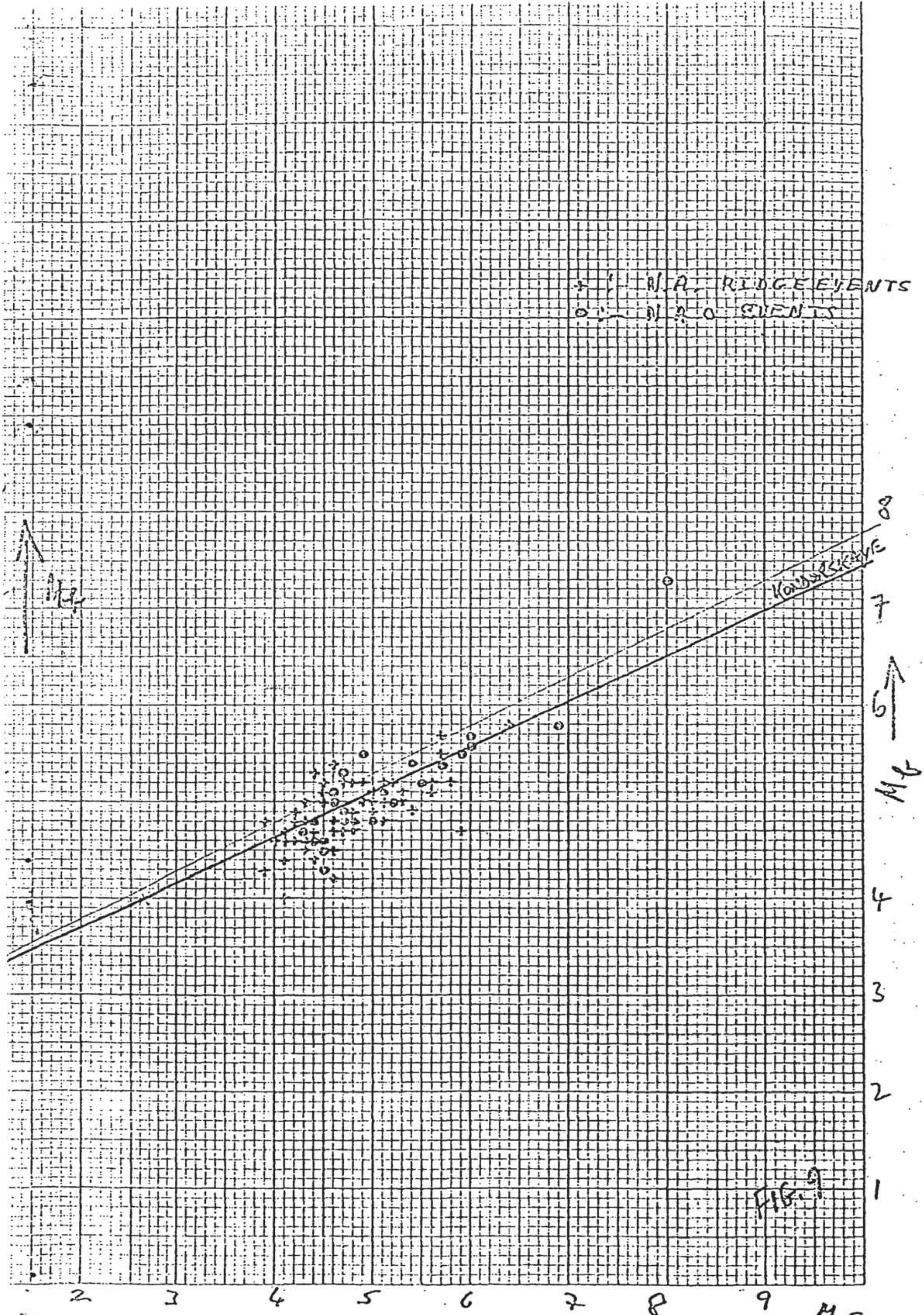
+ : N.A. RIDGE EVENTS
o : N.A.O EVENTS
KONDORSKAYA
Mb
2
3
4
5
6
7
8
9
MS
1
2
3
4
5
6
7
8

FIG. 9

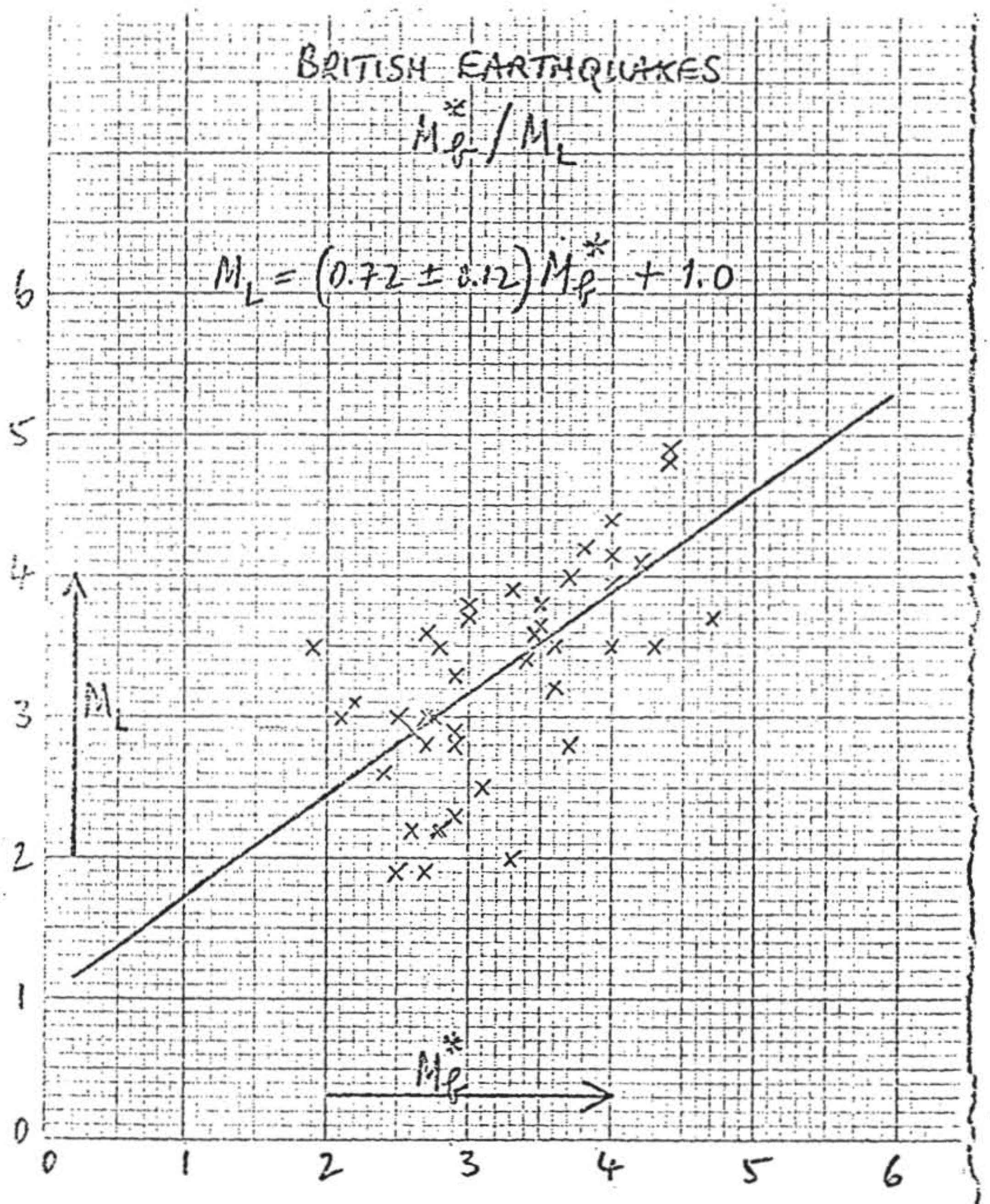

FIG. 10

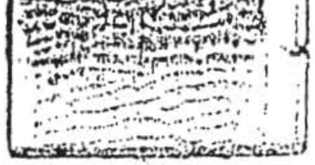

FIG. 12

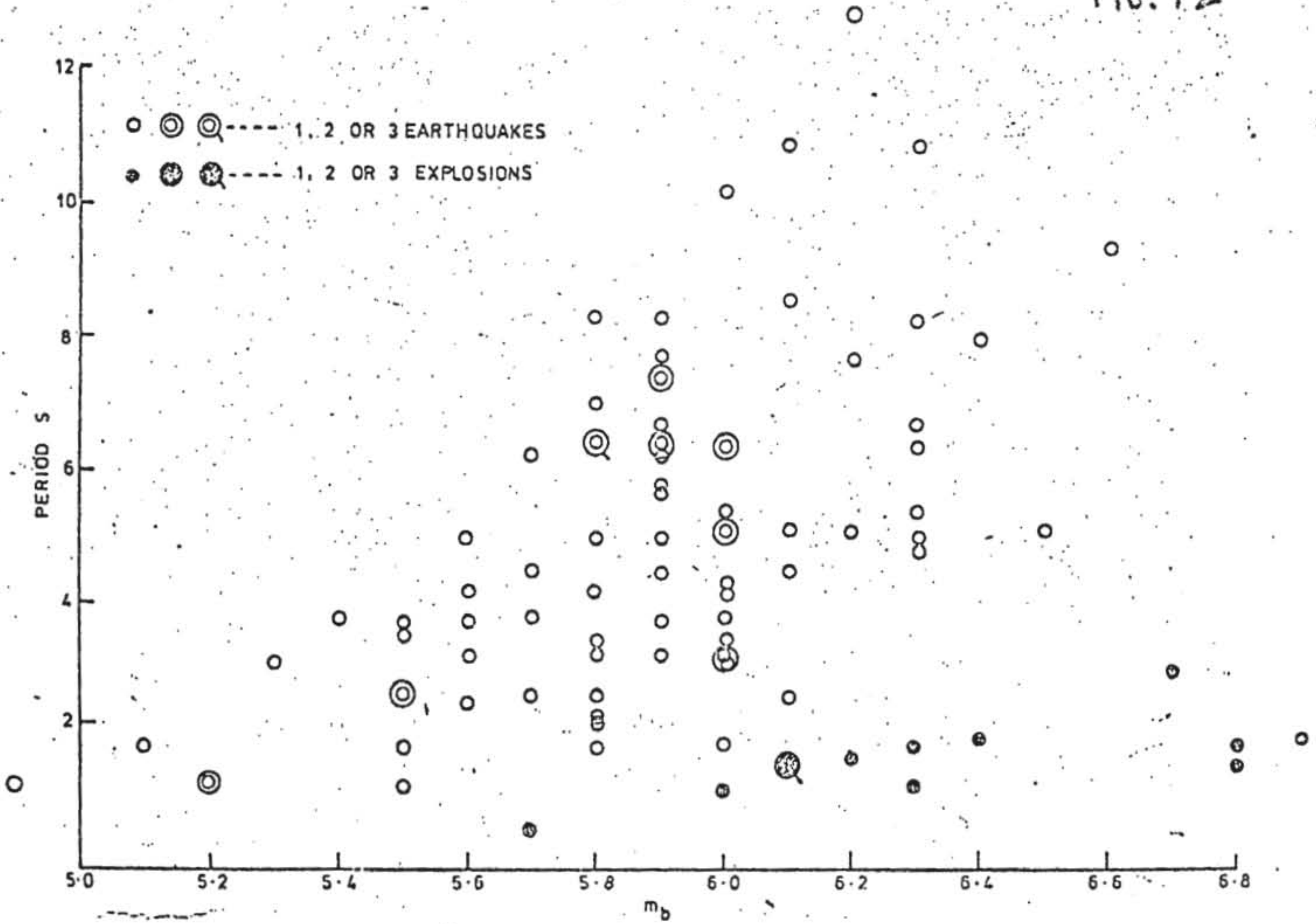

Crude discrimination between earthquakes and explosions using m_b (USCGS) v Dominant Period of the P wave

Source :

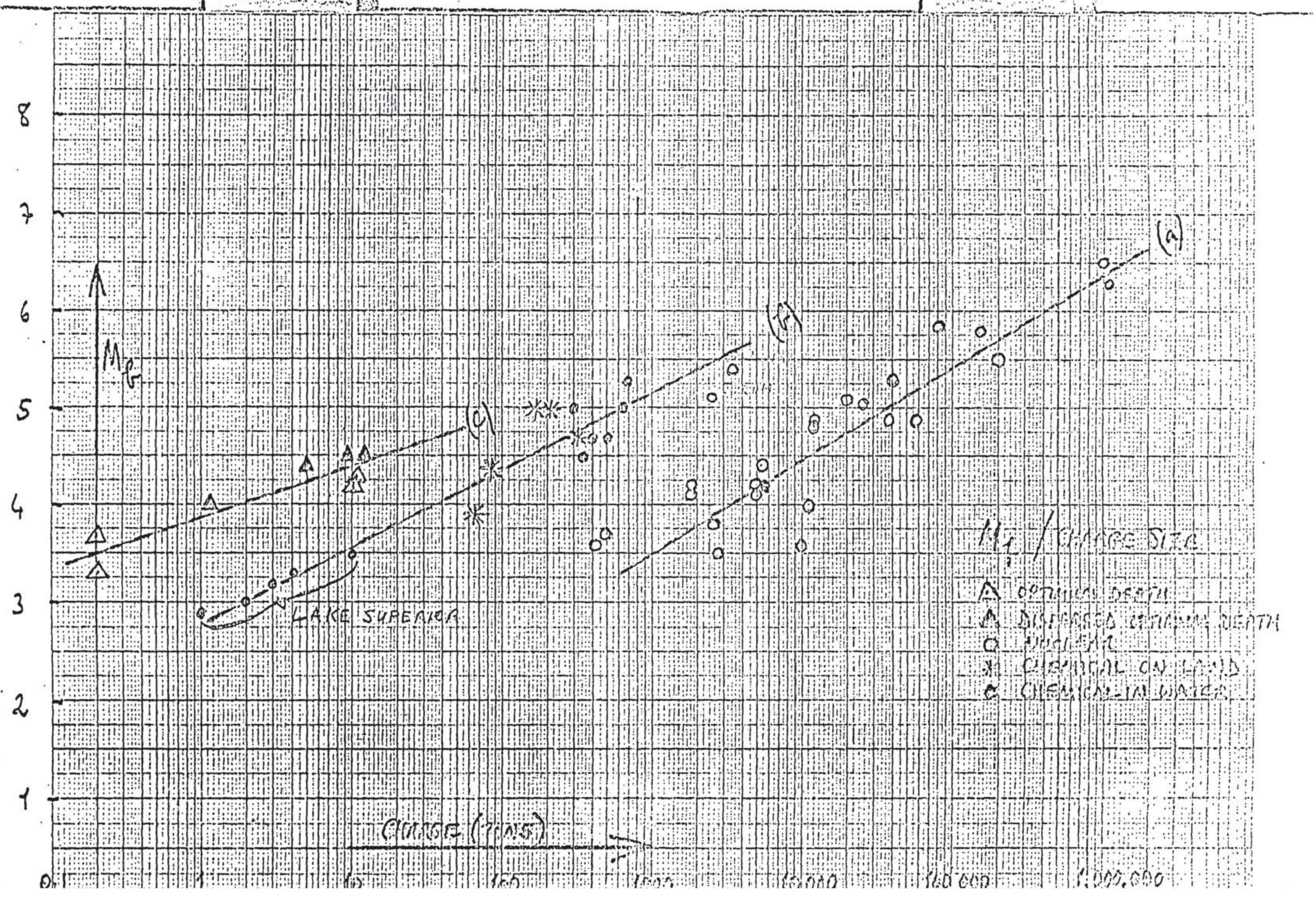
8
7
6
5
4
3
2
1
M_b
(a)
(b)
(c)
LAKE SUPERIOR
M_b / CHARGE SIZE
OPTIMUM DEPTH
DISPERSED OPTIMUM DEPTH
NUCLEAR
CHEMICAL ON LAND
CHEMICAL IN WATER
CHARGE (TONS)
0.1
1
10
100
1000
10,000
100,000
1,000,000

FIG 13

30/8/76

Graph Data Ref. 5551 Log 5 Cycles x mm, ½ and 1 cm

M_L vs Charge Size for Underwater Explosions

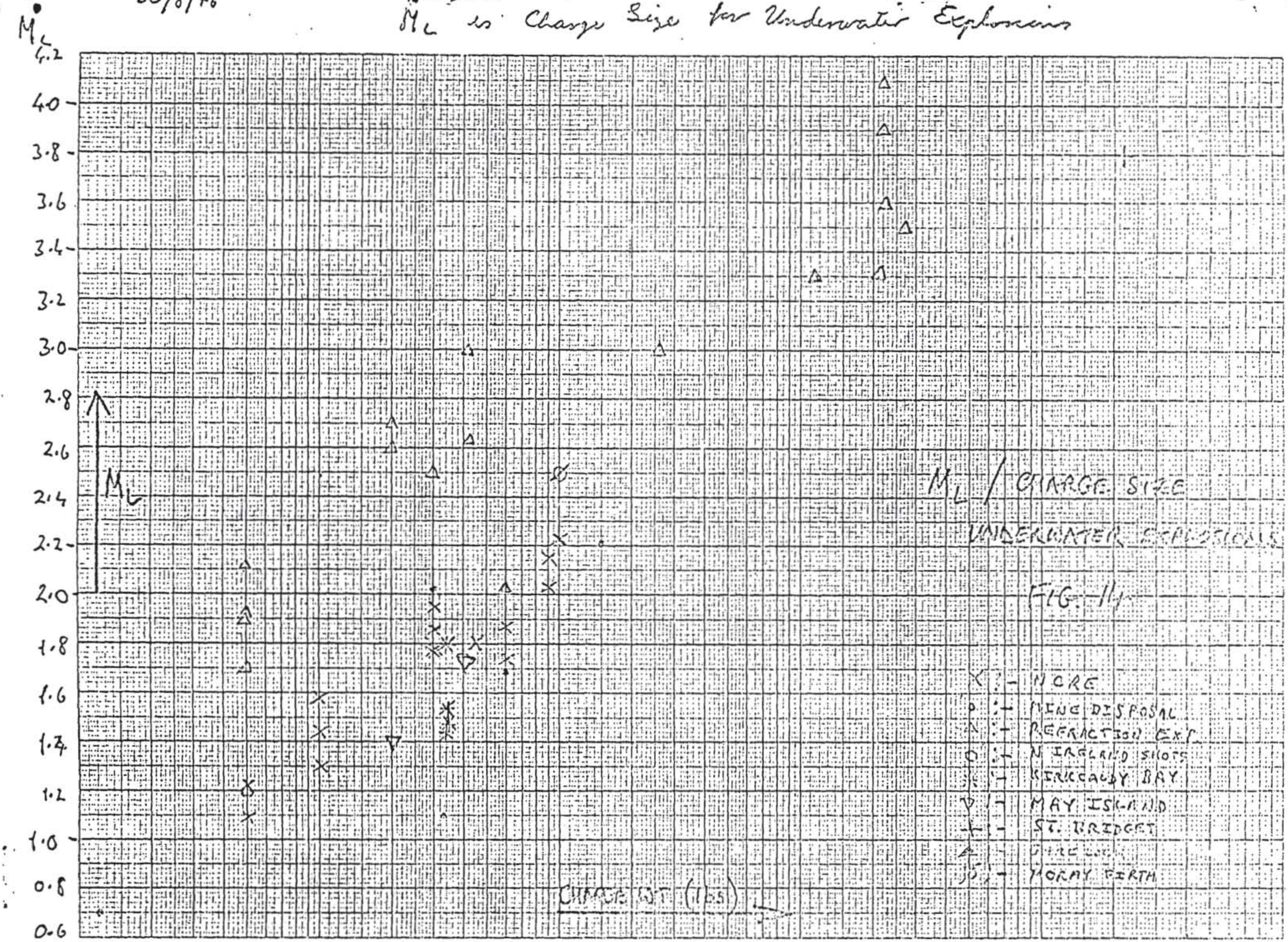

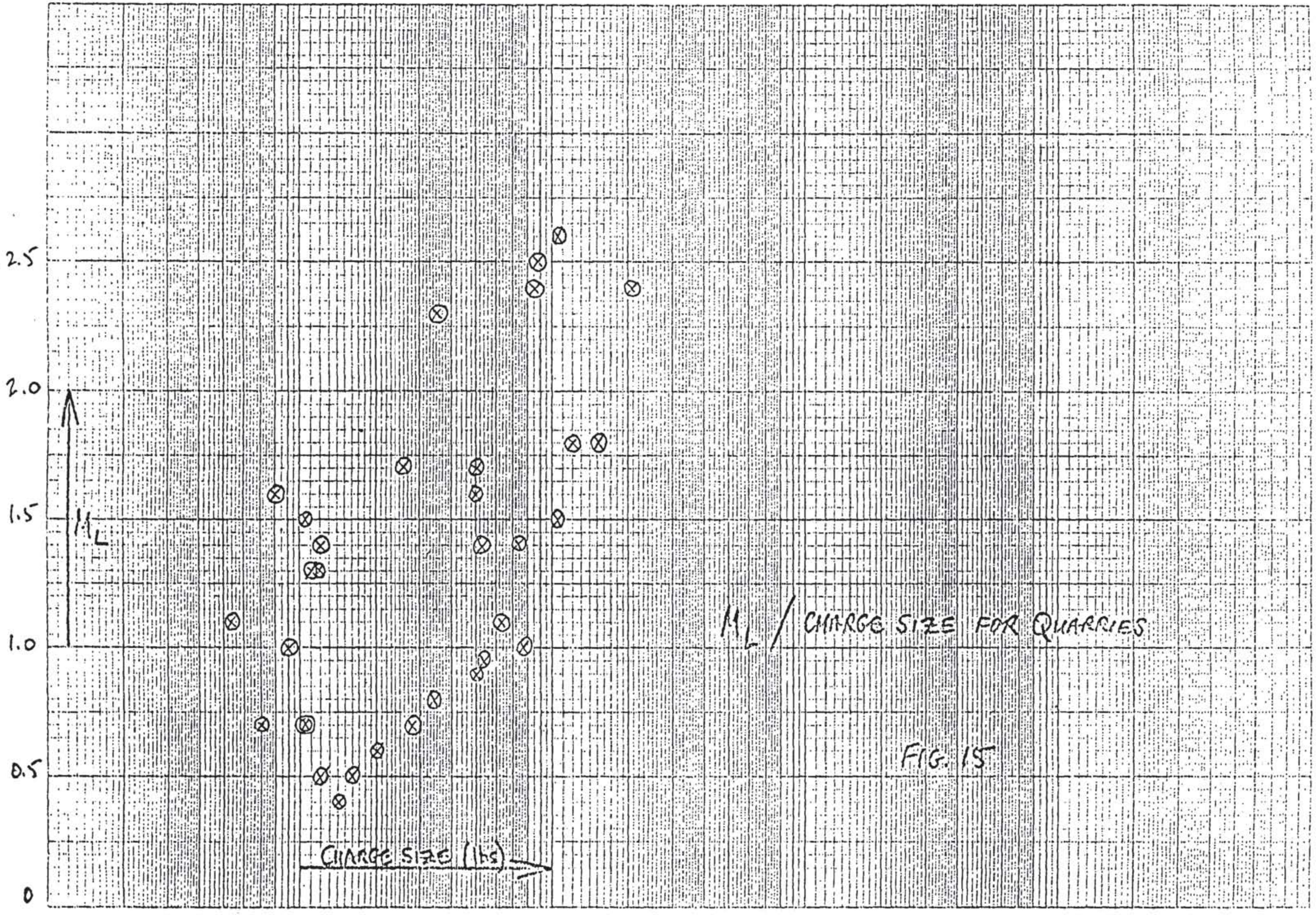

M_L / CHARGE SIZE FOR QUARRIES

FIG. 15